Computerized Analysis of Retinal Vessel Width and Tortuosity in Premature Infants

Clare M. Wilson,[1,2] *Kenneth D. Cocker,*[1] *Merrick J. Moseley,*[1] *Carl Paterson,*[3] *Simon T. Clay,*[3] *William E. Schulenburg,*[4] *Monte D. Mills,*[5,6] *Anna L. Ells,*[7] *Kim H. Parker,*[8] *Graham E. Quinn,*[5,6] *Alistair R. Fielder,*[1,2] *and Jeffrey Ng*[3]

Purpose. To determine, with novel software, the feasibility of measuring the tortuosity and width of retinal veins and arteries from digital retinal images of infants at risk of retinopathy of prematurity (ROP).

Methods. The Computer-Aided Image Analysis of the Retina (CAIAR) program was developed to enable semiautomatic detection of retinal vasculature and measurement of vessel tortuosity and width from digital images. CAIAR was tested for accuracy and reproducibility of tortuosity and width measurements by using computer-generated vessel–like lines of known frequency, amplitude, and width. CAIAR was then tested by using clinical digital retinal images for correlation of vessel tortuosity and width readings compared with expert ophthalmologist grading.

Results. When applied to 16 computer-generated sinusoidal vessels, the tortuosity measured by CAIAR correlated very well with the known values. Width measures also increased as expected. When the CAIAR readings were compared with five expert ophthalmologists' grading of 75 vessels on 10 retinal images, moderate correlation was found in 10 of the 14 tortuosity output calculations (Spearman $\rho = 0.618 - 0.673$). Width was less well correlated ($\rho = 0.415$).

Conclusions. The measures of tortuosity and width in CAIAR were validated using sequential model vessel analysis. On comparison of CAIAR output with assessments made by expert ophthalmologists, CAIAR correlates moderately with tortuosity grades, but less well with width grades. CAIAR offers the opportunity to develop an automated image analysis system for detecting the vascular changes at the posterior pole, which are becoming increasingly important in diagnosing treatable ROP.

From the [1]Department of Optometry and Visual Science, City University, Northampton Square, London, United Kingdom; [2]Department of Ophthalmology, St. Mary's Hospital, London, United Kingdom; the Departments of [3]Physics and [8]Bioengineering, Imperial College London, London, United Kingdom; [4]Department of Ophthalmology, Western Eye Hospital, London, United Kingdom; the [5]Division of Pediatric Ophthalmology, The Children's Hospital of Philadelphia, Philadelphia, Pennsylvania; [6]Scheie Eye Institute, University of Pennsylvania Health System, Philadelphia, Pennsylvania; and [7]Department of Surgery, Alberta Children's Hospital, Calgary, Alberta, Canada.

Supported by Action Medical Research (CMW) and The Particle Physics and Astronomy Research Council (SC, JN).

Submitted for publication October 19, 2007; revised January 4 and February 8, 2008; accepted June 19, 2008.

Disclosure: **C.M. Wilson**, None; **K.D. Cocker**, None; **M.J. Moseley**, None; **C. Paterson**, None; **S.T. Clay**, None; **W.E. Schulenburg**, None; **M.D. Mills**, None; **A.L. Ells**, Clarity Medical Systems (C); **K.H. Parker**, None; **G.E. Quinn**, None; **A.R. Fielder**, None; **J. Ng**, None

The publication costs of this article were defrayed in part by page charge payment. This article must therefore be marked "*advertisement*" in accordance with 18 U.S.C. §1734 solely to indicate this fact.

Corresponding author: Clare M. Wilson, Department of Optometry and Visual Science, City University, Northampton Square, London EC1V OHB, United Kingdom; clarewil25@yahoo.com.

(*Invest Ophthalmol Vis Sci.* 2008;49:3577–3585) DOI: 10.1167/iovs.07-1353

Progress in image analysis promises to revolutionize specific areas of medical practice and enable the quantification of signs that hitherto have been described only in a qualitative manner. Improved image acquisition and automated analysis have the potential to improve the cost effectiveness of retinal screening programs.

Retinovascular diseases are established candidates for this line of study, and diabetic retinopathy has been a focus of interest in the development of image analysis tools. A niche also exists for an automated technique for assessing the retina of the pediatric age group in infants at risk of retinopathy of prematurity (ROP).

ROP is categorized by zone and stage and by the presence of plus disease. Plus disease is an indicator of ROP severity and may present a constellation of signs including retinal arterial tortuosity and venous dilation at the posterior pole, vitreous haze, and iris rigidity. Plus disease is difficult to quantify, since the diagnosis is based on a 20-year-old reference photograph.[1] A reference photograph with less severe changes than that included in the International Classification of ROP (ICROP)[1] was used for treatment trials including the Multicenter Trial of Cryotherapy for ROP (CRYO-ROP)[2] and the Early Treatment of ROP randomized trial (ETROP).[3] Preplus disease, described as vascular abnormalities at the posterior pole that are insufficient to diagnose plus disease but that demonstrate more arterial tortuosity and venous dilation than normal, was added to the classification of ROP in 2005.[4] The diagnostic challenge that this disease presents is illustrated by the lack of interobserver repeatability of disease presence and absence by a panel of expert readers.[5,6]

To overcome the inherent inaccuracies in qualitative evaluation, several groups are exploring the use of automated techniques.[7–11] Various methods have been applied to retinal images, all of which use image segmentation to detect various parameters of the image automatically. Trials have been conducted on techniques of retinal image segmentation to localize retinal blood vessels for quantification such as vessel tracking, neural networking, and morphologic processing.[12] Imaging the retina in premature infants is considerably more challenging than in adult subjects. Factors such as cloudy media, small pupils, uneven illumination from an annular light source, and difficulty in examining an extremely preterm infant combine to limit the quality of the images obtained. Studies specifically aimed at analysis of the preterm retina have provided promising methods of vessel analysis,[7–11] yet none has advanced to the stage that it can be used as a reliable clinical tool.

One example of such vessel analysis software is Retinal Image multiScale Analysis (RISA), which is a method of blood vessel segmentation based on the scale space analysis of the first and second derivative of the intensity image, which gives information about its topology and overcomes the problem of variation in contrast in preterm infant retinal images.[13]

The ability to quantify the parameters of increasing vascular width and tortuosity specific to the development of plus disease of ROP has been proven with RISA.[9,10,13] Other similar software with slightly different methods of vessel localization and alternate methods for calculating tortuosity and width have been used to study the vasculature parameter changes and have shown them to be quantifiable.[7,8,14]

In this study, the performance of a novel computer analysis program, Computer-Aided Image Analysis of the Retina (CAIAR) (Ng et al., manuscript submitted) is assessed. It semiautomatically identifies the retinal vessels, with provision for human pixel editing if any vessels are inappropriately represented by CAIAR. It subsequently automatically measures the width and tortuosity of each vessel found. Segmentation of the digital image to localize arteries and veins is achieved using filtered detection measurements based on maximum likelihood estimation of vessel parameters from an image.

We have studied the accuracy of CAIAR vessel width and tortuosity determined by CAIAR in two ways: by providing the program with computer-generated sinusoidal model vessels of known width and both frequency and amplitude of tortuosity and by using digital images obtained from preterm infants who have had width and tortuosity of peripapillary vessels graded by experts.

METHODS

This study adhered to the tenets of the Declaration of Helsinki. Permission for usage of anonymous digital retinal images acquired from premature infants during routine screening was approved by St. Mary's Hospital Research and Development Department and University of Calgary Conjoint Health Research Ethics Board.

Program for Vessel Analysis of Digital Images

Vessel Localization. CAIAR computer software is under development at Imperial College London. The vessel-detection system is based on maximum likelihood model-fitting in a scale space framework. It employs filters that are sensitive to image structures at four different scales and models that are fitted to the filter outputs, to estimate the most likely vessel configuration. The estimated model of Gaussian profile, with parameters of height, width, and orientation are computed at each location in the image as illustrated in Figure 1. Finally, a verification stage is performed by measuring the contrast in a cross section perpendicular to the direction of the vessel and checking that the maximum contrast to the background is in the center of the proposed vessel. This measurement is obtained by using an isotropic second derivative of a Gaussian filter.

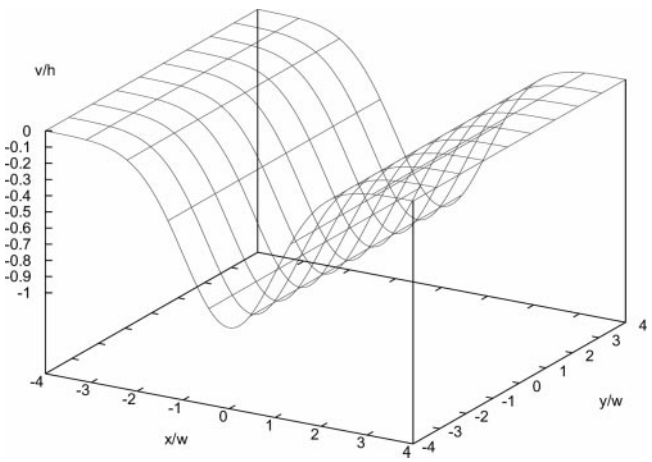

FIGURE 1. Illustration of the estimated model of Gaussian profile, with parameters of height, width and orientation computed at each location.

Vessel Tortuosity and Width. To measure tortuosity, the vessel centerline locations are grouped into contiguous structures by a connected component algorithm and each vessel is skeletonized to a 1-pixel thickness. Previous approaches to quantifying tortuosity have focused on measuring the bowing of a vessel from the ratio of the arc length (i.e., length along the vessel), to the chord length (i.e., straight-line distance between the two end points).[15] We adopted a multiscale approach that successively subdivides vessel sections into two parts. The geometric concept involves perpendicular bisection of the vessel chord at its midpoint and subsequent reapplication of the subdivision on the resultant segments until the segment lengths fall below a specified value (4 pixels). The concept is illustrated in Figure 2. Joining the end pixels of a vessel with a straight line gives chord length l_0 (Fig. 2A). The bisector of this line divides the vessel into two segments with subchord lengths of l_1 and l_2 (Fig. 2B). The two segments are each subdivided again to give four segments l_{11}, l_{12}, l_{21}, and l_{22} (Fig. 2B). Each application of subdivision across the vessel is called a level. We have two measures of local tortuosity: calculating the increase in chord length (Δl) from the division of the segment into two subsegments and calculating the increase in total chord length from one level of subdivision to another. Each of these two measures can be normalized, either by the chord length or the square of the chord length. Finally, we investigated the use of the maximum, mean, and sum of the normalized measures to give a total of 12 estimates of overall tortuosity. We also investigate two of the most promising formulas for tortuosity measures as proposed by Hart,[15] giving a total of 14 methods of calculating tortuosity.

Two methods were used to estimate width: First, we used the estimate from the maximum-likelihood model fitting. This is the standard deviation of the Gaussian profile that was fitted at that location. Second, we used the correlated measure of isotropic contrast at the vessel centerline, computed by the response of a Laplacian of Gaussian (LoG) filter.

Testing CAIAR Tortuosity and Width Measurements Using Model Vessels

The effectiveness of CAIAR was first tested on a series of model vessels computer generated by a program written in Java. The program generates a 246 × 246-pixel image of a 1-pixel-wide sinusoidal line by plotting the following formula for $20 < \times > 226$:

$$y = A \cdot \sin(f \cdot x/100) + 123$$

where A is the amplitude and $f/100$ is the frequency of the sinusoid, which is offset to appear in the center of the image.

Tortuosity. Modeled vessels of a frequency of 5, 10, and 20 pixels and amplitude of 2, 4, 6, and 8 pixels were created in all possible combinations.

Width. Width measurements were assessed directly from model straight vessels of widths from 1 to 10 pixels.

Both tortuosity and width vessel model images were analyzed by CAIAR, and the outcomes of 14 CAIAR tortuosity measurements and 2 CAIAR width measurements were analyzed.

Validation of Tortuosity and Width Measurements of Vessels on Clinical Digital Retinal Images by CAIAR

Digital retinal images obtained with a digital fundus camera (RetCam 130; Clarity Medical Systems Inc., Pleasanton, CA) during routine screening for ROP at St. Mary's Hospital (London, UK) and Alberta's Children's Hospital (Calgary, Alberta, Canada) were analyzed. Ten images were selected with a fair representation of wide and narrow, tortuous and straight vessels. The images were of adequate contrast quality for CAIAR analysis and visualization of the main artery and main vein in at least 3 quadrants was necessary for inclusion. Figures 3A and

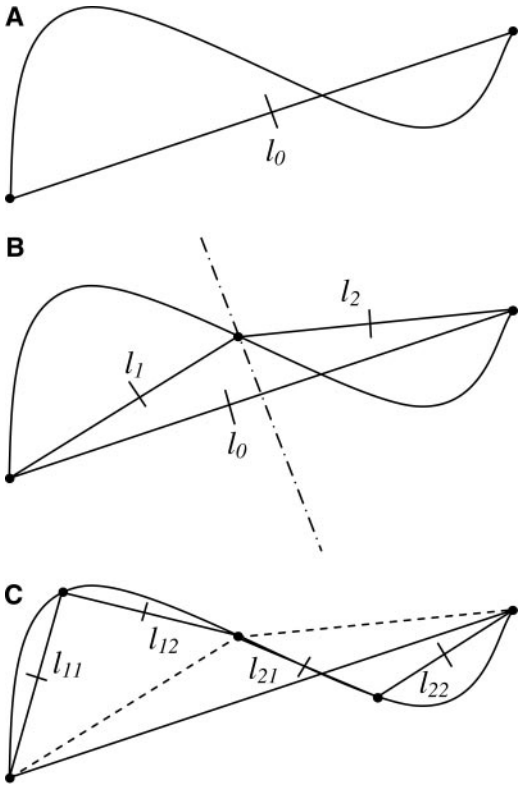

FIGURE 2. Vessel and its successive approximations after repeated perpendicular bisection of segments. (**A**) The chord length of a vessel segment; (**B**) a segment subdivided into two segments of chord lengths l_1 and l_2, by the bisector of the chord; (**C**) further subdivision of the two vessel segments from (**B**).

3B illustrate the diversity of vascular width and tortuosity in infants with and without ROP. Each image was cropped to 60° to prevent bias from viewing peripheral ROP changes (Fig. 4A).

These images were analyzed by the CAIAR software yielding tortuosity index (T) 1 to 14 (see the Appendix) and two widths for one vein and one artery in each quadrant of each image.

These 10 images were also graded by five expert ophthalmologists who regularly undertake ROP screening in ward rounds and have published papers on ROP. They each graded one vein and one artery from each quadrant of each image for tortuosity and width on an 11-point Likert scale (0–10).

The results of CAIAR software and the assessments by the experts were then compared for tortuosity and width of each artery and each vein on each of the 10 images, to validate the CAIAR values in a clinical setting.

Statistical Analysis

The frequency, amplitude, and width of model vessels were correlated to CAIAR output using the Spearman rank correlation test (ρ). The vessel width and tortuosity estimates obtained using CAIAR to analyze digital fundus images were rank correlated with the average grading by experts also using Spearman's ρ.

RESULTS

Validation of Tortuosity and Width Measurements of Model Vessels by CAIAR

Sixteen model vessels of differing amplitude and frequency were analyzed to examine the effectiveness of the measures of tortuosity in CAIAR. Table 1 shows the results of the 14 tortuosity readings from CAIAR (T_1– T_{14}) that were found to have perfect rank correlation when frequency and amplitude were varied as functions of each other. Table 1 reports amplitude increasing as a function of frequency and frequency increasing as a function of amplitude. The results indicate that as frequency and amplitude increase, so do the CAIAR tortuosity readings. T_1 to T_6 provided perfect ranking for all combinations of frequency and amplitude of model vessel tested and are suggested to be the most suitable tortuosity readings by CAIAR found thus far.

Figure 5 illustrates the increase in T_1 to T_6 with increasing frequency. Figure 5A shows the values for amplitude of 2 pixels, and Figure 5B shows the results for amplitude of 8 pixels. Each tortuosity value is expressed as a percentage of the highest frequency recorded; hence, all results at a frequency of 20 pixels have a value of 100%. (This method of displaying the results was chosen to avoid confusion from the extremes of scales used in each of the tortuosity results, which range from 0.003626 [T1 amplitude 2 pixels, frequency 5 pixels] to 0.015846 [T1 amplitude 2 pixels, frequency 20 pixels], to from 8.140222 [T6 amplitude 8 pixels, frequency 5 pixels], to 90.44195 [T6 amplitude 8 pixels, frequency 20 pixels].

Figure 6 shows the relation of the vessel width estimate calculated by CAIAR and the width (in pixels) of the model

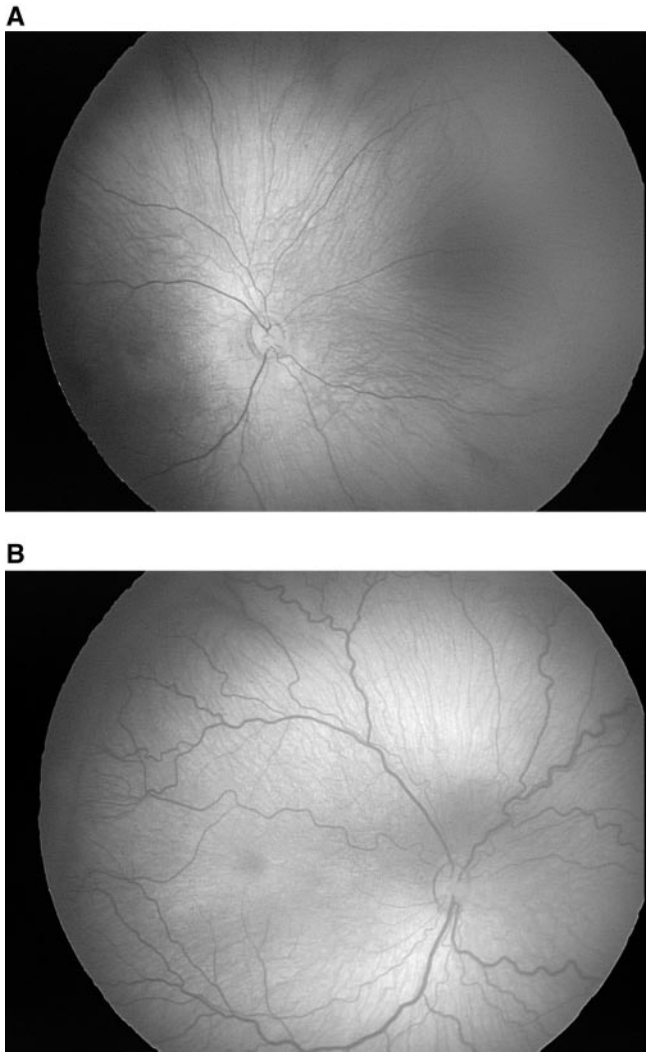

FIGURE 3. Retinal vasculature of preterm infants with and without ROP. (**A**) Digital retinal image to demonstrate vasculature of preterm infant without ROP. (**B**) Digital retinal image to demonstrate vasculature of an infant with ROP requiring treatment.

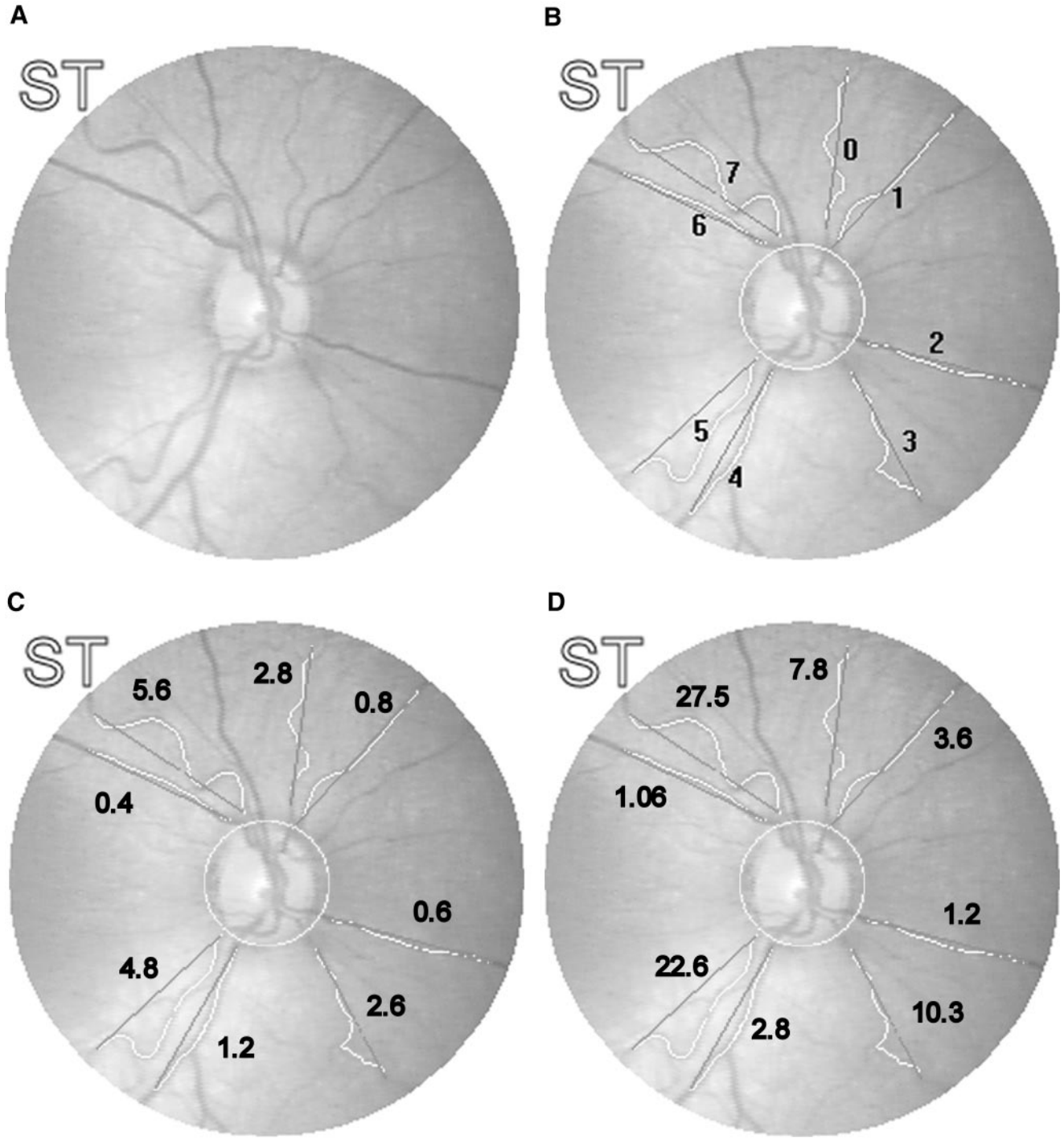

FIGURE 4. (**A**) Cropped RetCam image before automated analysis; (**B**) cropped RetCam image after automated analysis; (**C**) cropped RetCam image with average of expert grades superimposed to indicate degree of tortuosity; (**D**) cropped RetCam image after CAIAR analysis with T_6 values superimposed to indicate degree of tortuosity.

vessel under analysis. Figure 7 shows the relation of the LoG contrast calculated by CAIAR and the width in pixels of the model vessel under analysis. Five model vessels in the range of 1 to 10 pixels wide were analyzed. For example, 1 pixel is calculated as 0.5, 3 pixels as 1.1, and 5 pixels as 2.5. Since most vessels are in the range 2 and 5 pixels wide the results of this analysis will demonstrate a reliably reported increase in vessel width. In addition, the similarity of the readings in the higher pixel range is unlikely to have clinical significance. The nonlinear relation is a result of the finite range of scales used in the scale space analysis of CAIAR.

Comparison of Tortuosity and Width Measurements of Vessels on Digital Retinal Images by CAIAR with Grading by ROP Experts

Ten digital images obtained from preterm infants were analyzed by quadrant, assessed for tortuosity and width. A total of

TABLE 1. Model Vessel Validation of CAIAR Tortuosity Readings

Frequency	Amplitude	T1	T2	T3	T4	T5	T6	T7	T8	T9	T10	T11	T12	T13	T14
Amplitudes as a Function of Frequency															
5	2,4,6,8	O	O	O	O	O	O	X	X	X	X	X	X	X	X
10	2,4,6,8	O	O	O	O	O	O	O	O	O	X	O	O	O	O
15	2,4,6,8	O	O	O	O	O	O	O	O	O	O	O	X	O	O
20	2,4,6,8	O	O	O	O	O	O	O	O	O	O	O	O	X	X
Frequencies as a Function of Amplitude															
5, 10, 15, 20	2	O	O	O	O	O	O	O	O	O	X	O	O	X	X
5, 10, 15, 20	4	O	O	O	O	O	O	O	O	O	O	X	X	O	O
5, 10, 15, 20	6	O	O	O	O	O	O	O	O	O	X	O	O	O	O
5, 10, 15, 20	8	O	O	O	O	O	O	O	O	O	O	O	O	O	O

Rank correlation of frequency and amplitude (subunits of tortuosity), showing which of 14 tortuosity indices had a perfect ranking. O, perfect rank correlation; X, imperfect rank correlation.

75 vessels were localized and measured for width and tortuosity with the CAIAR software. Figure 4 illustrates the analysis for one such image. Figure 4A shows the preanalysis image. It is a cropped digital fundus image from an infant born at 27 weeks of gestational age with a birth weight of 950 g and who had stage 3 ROP that was subsequently treated with laser panretinal photocoagulation. Figure 4B shows the postanalysis image.

The tortuosity result for each of the eight vessels, as designated by the expert graders, is illustrated superimposed on the original image in Figures 4C, and Figure 4D shows superimposed CAIAR tortuosity results. At this point, the vessel analysis program does not distinguish between arteries and veins and may pick up more or fewer than two vessels per quadrant. This analysis can be edited manually to allow no more than two vessels to be analyzed per quadrant.

Table 2 shows the correlations for tortuosity with grades from experts in ROP. All were statistically significant ($P < 0.0001$), ranging from $\rho = 0.492$ for T14 to $\rho = 0.673$ for calculation T9.

Another feature of ROP is increased vessel width, as shown by increasing width of the veins of plus disease of ROP.[1] The original measure of width developed by CAIAR does not correlate significantly with the average expert readers' clinical assessment ($\rho = -0.113$, $P < 0.334$). However, the LoG output which is based solely on image contrast rather than any geometric property, reveals a moderate but statistically significant correlation with width grades from the experts ($\rho = 0.415$, $P < 0.0001$).

DISCUSSION

CAIAR has already been shown able to detect retinal vessels reliably and the output can be optimized via an editing facility. In this report, the vessel model constructs have verified the integrity of CAIAR using models to demonstrate that it recognizes the increase in pixel width measurements and two of the major characterizing features of tortuosity: frequency and amplitude.

We have also demonstrated that tortuosity can be measured automatically from digital retinal images by using CAIAR, and from the model it can be extrapolated that it can be measured across a wide range of amplitudes and frequencies. With CAIAR, it is possible to detect small changes in frequency and amplitude, and 10 of the 14 tortuosity measures tested correlate well with the clinician's grading.

Image capture in preterm infants is a challenge in itself. Undoubtedly, not all images acquired by the fundus camera (RetCam 130; Clarity Medical Systems Inc.) are of adequate quality for analysis. In routine practice, we have adopted a five-image protocol in which the first image has the optic disc at its center. (This image is used as a baseline for image quality with respect to focusing and illumination.) When this image has been obtained, the remaining four peripheral images are captured.[16] In our experience, it is rare not to have an adequate posterior pole image from both eyes of each infant screened. The incidence of poor-quality images is far higher when viewing the peripheral retina.

Width changes are difficult to detect accurately on digital images with automated systems, since width estimates are sensitive to the imaging process and are likely to be more affected by poor image quality—an inherent problem when imaging premature infants—than are tortuosity measures. A 10% change in width is more difficult to detect than a similar change in tortuosity. Width changes measured by CAIAR and compared with expert grader readings correlate very poorly. This may be the result of image-quality limitations, or could be due to shortcomings in the observer grading system. As it is challenging for a computer program to distinguish the accuracy of vessel width, so it may also be challenging for the human eye to be sensitive to such small changes. As there is no gold standard for plus disease assessment, inaccuracies are also likely to develop in assessing a new grading system.[17] Chapman et al.[18] compared the sensitivity of various methods of measuring retinal width. They found the sliding linear regression filter to be more accurate, compared to Gaussian profile fitting. They also tested a standard edge detection algorithm, which was the least accurate.

Images captured by the another fundus camera (NM200D; Nidek, Inc., Aichi, Japan) were analyzed with vascular imaging semiautomated software (VesselMap; Imedos, Jena, Germany), to estimate retinal vessel diameter to a level sufficient to observe a significant increase in retinal vein diameter with plus disease compared to that without plus disease.[19] The vascular imaging software has also shown a significant decrease in retinal vein and artery diameters after laser treatment of ROP.[20] The increased resolution of the NM200D images (Nidek) may explain the success of this system; however, the dichotomous detection found to be significant in these papers is somewhat less challenging than the grading system we are developing with CAIAR.

CAIAR tortuosity readings T_{1-6} correlate well with increasing amplitude and frequency of computer-generated lines with perfect rank correlation. As these parameters are suggestive of increasing tortuosity, it may be expected that these same six tortuosity readings would give the best correlations with expert clinical grading. Indeed, the results of T_{1-6} show good correlation with clinical grading, yet T_{7-12} also have good correlation, with T_9 having the highest correlation. This finding suggests that the ophthalmologists' notion of tortuosity is not based solely on regular amplitude and frequency changes. The

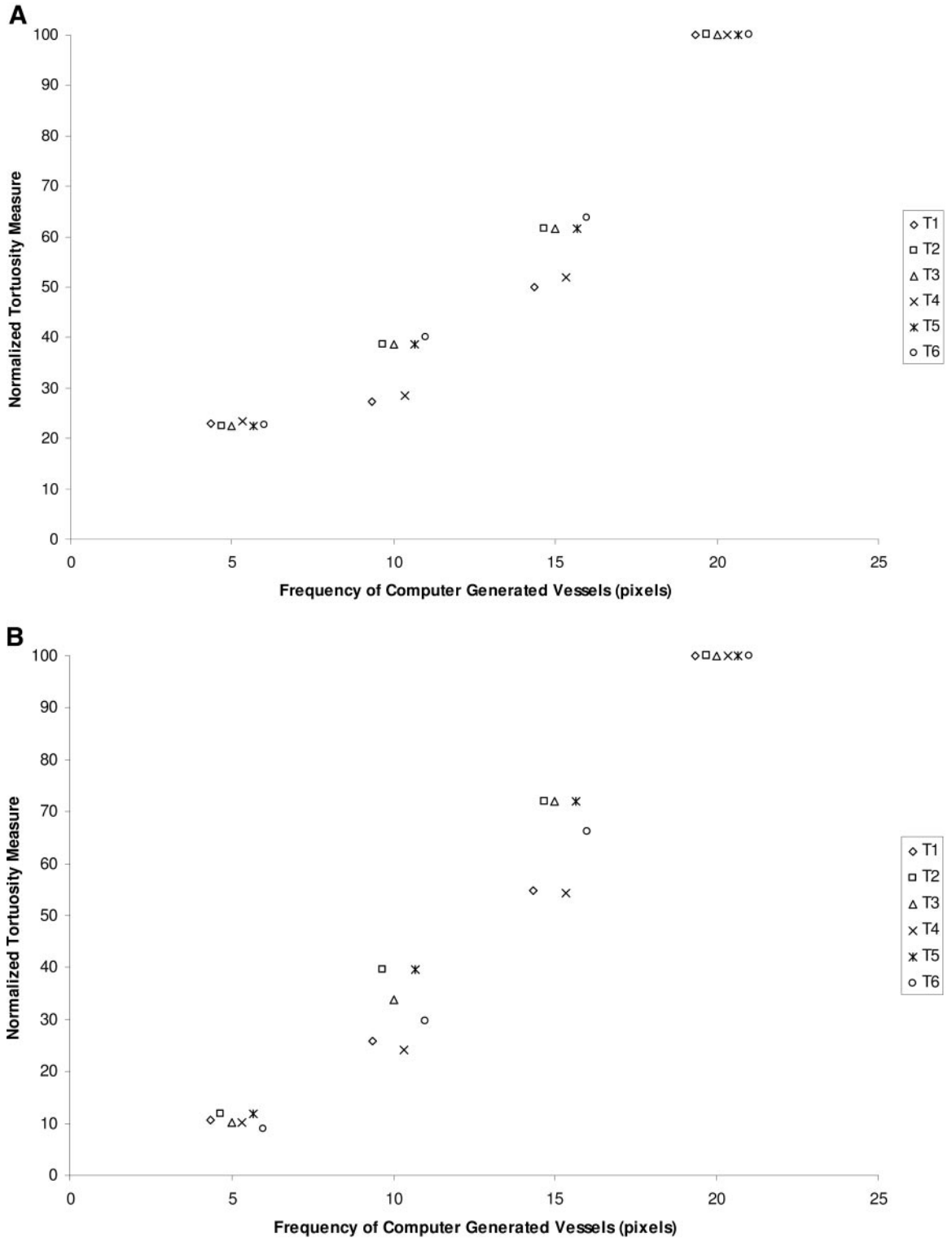

FIGURE 5. Relation of tortuosity expressed as a percentage versus frequency; frequency 5, 10, 15 and 20—results spread on abcissa for clarity. (**A**) Amplitude constant at 2 pixels; and (**B**) amplitude constant at 8 pixels

computer generated vessels analyzed were all uniform in their sinusoids; however, retinal vessels are not so well proportioned. The somewhat unexpectedly higher results for the formulas less well correlated by model vessel analysis (Tables 1, 2) may be in part explained by a higher level of processing by a human observer enabling more complex judgment of less uniform vessels than the computerized system. These results also suggest that T_{7-12} equations are closer to the human perception of tortuosity—a far-from-defined entity. These equations are all based on segment-wise tortuosity measures compared with the level-wise measures of T_{1-6}. The significance of the segment-wise derivations is that they use the local increase in total chord length from one segment into two, as opposed to the total increase in chord length from one level to another to approximate

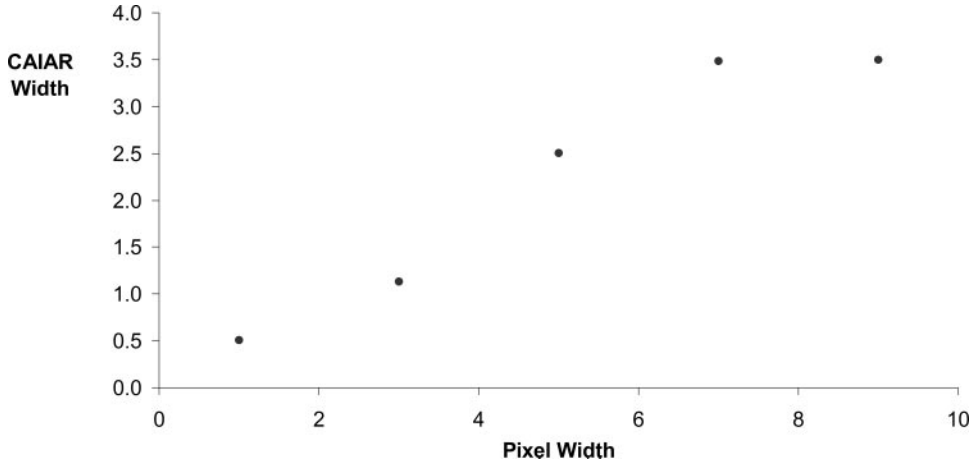

FIGURE 6. Relation of pixel count of model vessel analyzed and width reported by CAIAR.

tortuosity, which appears to be more akin to the ophthalmologists' conception of tortuosity (see the Appendix).

The tortuosity indices derived from the formulas of Hart et al.[15] (T_{13} and T_{14}) are less well correlated with both model vessel output and clinical expert grades than are T_{1-12}. The published high receiver operating curve characteristics of these formulas to clinical judgment may have been artificially high, because the vessels were only assessed as a dichotomy: tortuous and nontortuous. The more robust testing of their formulas on our finer scale suggests that it is less well suited to clinical tortuosity grading than is T_{1-12}.

The problem of defining tortuosity is not a trivial one. We have found more than six mathematical definitions of tortuosity in the literature, all giving slightly different results for different controlled examples of tortuosity (e.g., sinusoidal, helical, and random). The algorithm has been expanded to calculate all the different mathematical derivations, but there is not yet agreement about what experts mean by tortuosity and hence no way to decide which of many measures fit best with the experts' evaluations.

Although the diagnosis of plus disease is currently challenging, its importance as realized in the ETROP randomized trial cannot be ignored, and the present results suggest that these vascular changes are now important in grading ROP and are a major factor in decisions about ROP treatment.[3] Unlike the peripheral ROP lesions, which require indirect ophthalmoscopy, the changes in plus disease, because they occur in the posterior pole region, are easier to detect by alternative examination techniques including digital imaging. The vascular changes located at the posterior pole therefore offer great hope of a grading tool that would enable grading to be performed uniformly and reproducibly and facilitate staging remotely by a nonophthalmologist, thereby opening up realistic screening programs, even in those areas where ophthalmic expertise is limited. It has already been shown that nonophthalmologists can successfully acquire digital images adequate for use in a screening program.[21,22]

Other analysis tools have been used with digital images to quantify and grade plus disease in infants at risk for ROP. The output from RISA has been tested in two previous reports.[9,10] One showed a trend for increasing venous and arterial width and significant increase in arterial tortuosity with increasingly severe ROP.[9] The other showed a significant increase in arterial and venous tortuosity and width in images with plus disease compared with those without plus disease.[10] Vessel width has also been shown to be increased by 15% in plus compared to no plus images using vascular analysis software (VesselMap; Imedos), a less automated system developed purely for width measurement.[19]

ROPtool, developed in the Duke Eye Center (Durham, NC), uses centerline extraction to model tubular objects on an image and thereby to localize and quantify retinal vasculature in preterm infants. Wallace et al.,[7] using this method, report a 95% sensitivity and 78% specificity for diagnosing tortuosity significant for plus disease compared with two expert readers' assessments.

A difference in the tortuosity (1.125 vs. 1.097, significant at 95% level) and width (96.8 vs. 86.4, significant at 99% level) measurements have also been illustrated between those infants who did and those who did not require treatment for ROP,

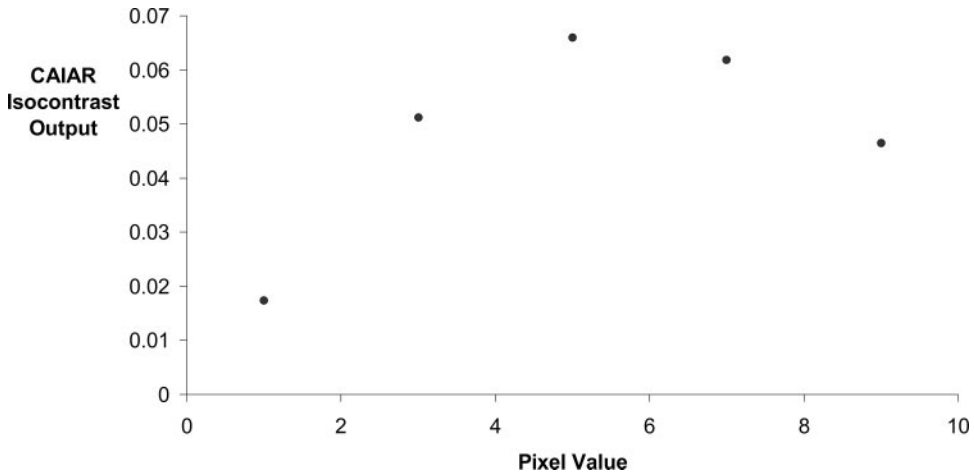

FIGURE 7. Relation of pixel count of model vessel analyzed and Laplacian of Gaussian (LoG) measure reported by CAIAR.

TABLE 2. Correlation for CAIAR Tortuosity Index (T) and Average of Expert Vessel Tortuosity Grading

T	Correlation Coefficient (Spearman ρ)
T_1	0.569
T_2	0.618
T_3	0.620
T_4	0.591
T_5	0.618
T_6	0.631
T_7	0.652
T_8	0.670
T_9	0.673
T_{10}	0.629
T_{11}	0.661
T_{12}	0.651
T_{13}	0.503
T_{14}	0.492

For all, $P < 0.0001$.

according to a semiautomated program developed in Dublin.[8] The segmentation technique for localization of vasculature in this program involves morphologic processing to emphasize linear structures, a second derivative operator that helps define thin structures, and a final morphologic filtering stage.[8]

Another group based in Thailand has developed an algorithm specifically for RetCam130 images (Clarity Medical Systems, Inc.). The program uses a statistically optimized LoG filter for image edge detection, followed by medial axis skeletonization and Otsu's thresholding algorithm for production of a binary image. The resultant image is then pruned and undergoes iterative spur removal.[11]

The ability of observers to discern clinically relevant increments in blood vessel diameter and tortuosity is considerable.[23] However, agreeing on the presence or absence of plus disease provides a greater challenge.[5] This is probably at least in part because there is no gold standard for plus disease measurement, and when a "fuzzy gold standard" is used, test accuracy can be greatly affected.[17] With advancing digital imaging techniques it has been possible to quantify the changes of vessel width and tortuosity associated with various parameters of ROP.[7–10,19] Unlike current subjective clinical standards based on comparison with an image, automatic image analysis of vascular tortuosity could provide a more ideal reproducible, objective, and standardized way of grading ROP. Automated screening tools could also enable a swift advancement in the possibilities of ophthalmic telemedicine and remote monitoring and grading. ROP has already been proven a suitable disease for telemedicine applications.[24] Further research applications of CAIAR and other retinal vessel analysis tools would be in studying retinal vessel changes in animal models of ROP. This has been successfully used to investigate the potential of rod photoreceptor function in predicting the blood vessel abnormalities in ROP.[24] This study demonstrates the feasibility of the CAIAR analytic software in grading the tortuosity and width of model vessels and demonstrates correlation of CAIAR measurements to expert grading of actual images of infants at risk for ROP, leading toward a simple clinical tool for diagnosing plus disease of ROP within the foreseeable future.

APPENDIX

Equations for 14 Tortuosity Measures

The increase in chord length resulting from dividing a vessel segment (s) into two subsegments provides a measure of tortuosity and is defined as

$$\Delta l_s = l_{c1(s)} + l_{c2(s)} - l_s.$$

where c1(s) and c2(s) are the two subsegments.

The total chord length at each level or step of subdivision over the whole vessel (e.g., 1, 2, 4, 8 segments), is given by

$$L_i = \sum_{s \in \text{level}(i)} l_s,$$

where level(i) is the set of all segments at level of subdivision i.

The tortuosity across the whole vessel caused by the increasing levels of subdivision is given by

$$\Delta L_i = L_{i+1} - L_i.$$

Finally, the two measures are either normalized by the chord length(s) or the square of the (sum of) the chord length(s).

During subdivision of a segment, the subsegments with chord lengths that are less than 4 pixels are rejected, and further subdivision is stopped for that subsegment. At the end of the subdivision process, there are N subsegments and M layers. We derived 12 different measures of overall vessel tortuosity, as follows:

	Aggregation Function	Tortuosity Measurement	Normalization
1. $v_1 = \max_i\left(\frac{\Delta L_i}{L_i}\right)$	Max	Level-wise	L
2. $v_2 = \frac{1}{M}\sum_i^M\left(\frac{\Delta L_i}{L_i}\right)$	Mean	Level-wise	L
3. $v_3 = \sum_i^M\left(\frac{\Delta L_i}{L_i}\right)$	Sum	Level-wise	L
4. $v_4 = \max_i\left(\frac{\Delta L_i}{(L_i)^2}\right)$	Max	Level-wise	L^2
5. $v_5 = \frac{1}{M}\sum_i^M\left(\frac{\Delta L_i}{(L_i)^2}\right)$	Mean	Level-wise	L^2
6. $v_6 = \sum_i^M\left(\frac{\Delta L_i}{(L_i)^2}\right)$	Sum	Level-wise	L^2
7. $v_7 = \max_s\left(\frac{\Delta l_s}{l_s}\right)$	Max	Segment-wise	l
8. $v_8 = \frac{1}{N}\sum_s^N\left(\frac{\Delta l_s}{l_s}\right)$	Mean	Segment-wise	l
9. $v_9 = \sum_s^N\left(\frac{\Delta l_s}{l_s}\right)$	Sum	Segment-wise	l
10. $v_{10} = \max_s\left(\frac{\Delta l_s}{(l_s)^2}\right)$	Max	Segment-wise	l^2
11. $v_{11} = \frac{1}{N}\sum_s^N\left(\frac{\Delta l_s}{(l_s)^2}\right)$	Mean	Segment-wise	l^2
12. $v_{12} = \sum_s^N\left(\frac{\Delta l_s}{(l_s)^2}\right)$	Sum	Segment-wise	l^2

We also provide two of Hart's best-performing tortuosity measurements[15] as a comparison,

$$\kappa(t) = \frac{x'(t)y''(t) - x''(t)y'(t)}{[y'(t)^2 + x'(t)^2]^{3/2}}$$

$$13. \quad \tau_6 = \int_{t_0}^{t_1} |\kappa(t)| dt / l_0$$

$$14. \quad \tau_7 = \int_{t_0}^{t_1} \kappa(t)^2 dt / l_0.$$

References

1. The Committee for the Classification of Retinopathy of Prematurity. An international classification of retinopathy of prematurity. *Arch Ophthalmol*. 1984;102(8):1130–1134.
2. Cryotherapy for Retinopathy of Prematurity Cooperative Group. Multicenter trial of cryotherapy for retinopathy of prematurity: preliminary results. *Arch Ophthalmol*. 1988;106(4):471–479.
3. Early Treatment for Retinopathy of Prematurity Cooperative Group. Revised indications for the treatment of retinopathy of prematurity: results of the early treatment for retinopathy of prematurity randomized trial. *Arch Ophthalmol*. 2003;121(12):1684–1694.
4. The Committee for the Classification of Retinopathy of Prematurity. The international classification of retinopathy of prematurity revisited. *Arch Ophthalmol*. 2005;123(7):991–999.
5. Chiang MF, Jiang L, Gelman R, et al. Interexpert agreement of plus disease diagnosis in retinopathy of prematurity. *Arch Ophthalmol*. 2007;125(7):875–880.
6. Reynolds JD, Dobson V, Quinn GE, et al. Evidence-based screening criteria for retinopathy of prematurity: natural history data from the CRYO-ROP and LIGHT-ROP studies. *Arch Ophthalmol*. 2002; 120(11):1470–1476.
7. Wallace DK, Zhao Z, Freedman SF. A pilot study using "ROPtool" to quantify plus disease in retinopathy of prematurity. *J AAPOS*. 2007;11(4):381–387.
8. Heneghan C, Flynn J, O'Keefe M, et al. Characterization of changes in blood vessel width and tortuosity in retinopathy of prematurity using image analysis. *Med Image Anal*. 2002;6(4):407–429.
9. Swanson C, Cocker KD, Parker KH, et al. Semiautomated computer analysis of vessel growth in preterm infants without and with ROP. *Br J Ophthalmol*. 2003;87(12):1474–1477.
10. Gelman R, Martinez-Perez ME, Vanderveen DK, et al. Diagnosis of plus disease in retinopathy of prematurity using Retinal Image multiScale Analysis. *Invest Ophthalmol Vis Sci*. 2005;46(12): 4734–4738.
11. Sukkeaw L, Barman UB, Fielder SA, Cocker K. Automatic extraction of the structure of the retinal blood vessel network of premature infants. *J Med Assoc Thailand*. 2007;90(8):1780–1792.
12. Patton N, Aslam TM, MacGillivray T, et al. Retinal image analysis: concepts, applications and potential. *Prog Retin Eye Res*. 2006; 25(1):99–127.
13. Martinez-Perez ME, Hughes AD, Stanton AV, et al. Retinal vascular tree morphology: a semi-automatic quantification. *IEEE Trans Biomed Eng*. 2002;49(8):912–917.
14. Wallace DK, Jomier J, Aylward SR, et al. Computer-automated quantification of plus disease in retinopathy of prematurity. *J AAPOS*. 2003;7(2):126–130.
15. Hart WE, Goldbaum M, Cote B, et al. Measurement and classification of retinal vascular tortuosity. *Int J Med Inform.* 1999;53(2–3):239–252.
16. Balasubramanian M, Capone A Jr, Hartnett ME, et al. The Photographic Screening for Retinopathy of Prematurity Study (Photo-ROP): study design and baseline characteristics of enrolled patients. *Retina*. 2006;26(7 suppl):S4–S10.
17. Phelps CE, Hutson A. Estimating diagnostic test accuracy using a "fuzzy gold standard". *Med Decis Making*. 1995;15(1):44–57.
18. Chapman N, Witt N, Gao X, et al. Computer algorithms for the automated measurement of retinal arteriolar diameters. *Br J Ophthalmol*. 2001;85(1):74–79.
19. Johnson KS, Mills MD, Karp KA, et al. Semiautomated analysis of retinal vessel diameter in retinopathy of prematurity patients with and without plus disease. *Am J Ophthalmol*. 2007;143(4):723–725.
20. Johnson KS, Mills MD, Karp KA, et al. Quantitative analysis of retinal vessel diameter reduction after photocoagulation treatment for retinopathy of prematurity. *Am J Ophthalmol*. 2007;143(6): 1030–1032.
21. Yen KG, Hess D, Burke B, et al. Telephotoscreening to detect retinopathy of prematurity: preliminary study of the optimum time to employ digital fundus camera imaging to detect ROP. *J AAPOS*. 2002;6(2):64–70.
22. Skalet AH, Quinn GE, Ying GS, et al. Telemedicine screening for retinopathy of prematurity in developing countries using digital retinal images: a feasibility project. *J AAPOS.* Published online February 19, 2008.
23. Freedman SF, Kylstra JA, Capowski JJ, et al. Observer sensitivity to retinal vessel diameter and tortuosity in retinopathy of prematurity: a model system. *J Pediatr Ophthalmol Strabismus*. 1996;33(4):248–254.
24. Ells AL, Holmes JM, Astle WF, et al. Telemedicine approach to screening for severe retinopathy of prematurity: a pilot study. *Ophthalmology*. 2003;110(11):2113–2117.